



Remotely Sensed Methodologies for Crop Water Availability and Requirements in Precision Farming of Vulnerable Agriculture

Nicolas R. Dalezios^{1,2} · Nicholas Dercas² · Nicos V. Spyropoulos³ · Emmanouil Psomiadis² 

Received: 1 December 2017 / Accepted: 4 December 2018 /

Published online: 4 January 2019

© Springer Nature B.V. 2019

Abstract

Agriculture is mainly impacted by water availability. Differences in climate conditions and the appearance of severe events, like droughts, has a significant imprint on local, regional and global agricultural productivity. The goal of this paper is to present remotely sensed approaches for water availability and requirements in vulnerable agriculture. Earth Observation (EO) data contribute to precision agriculture for efficient crop monitoring and irrigation management. A drought susceptible region considered as vulnerable farming was chosen, in the Thessaly prefecture in Central Greece. Water availability is measured by means of precipitation frequency examination and drought estimation. Crop water requirements are measured by assessing crop evapotranspiration (ET) with the synergistic use of WV-2 satellite images and ground-truth data. The remote-based ET_{csat} is assessed by utilizing the reference ET_o derived from Food and Agriculture Organization (FAO) methodology, while the meteorological data and K_c are evolved from Normalized Difference Vegetation Index (NDVI). According to the rainfall frequency studies, indicators demonstrate a significant precipitation decrease. The results reveal the importance of water availability estimation for facing agriculture water needs and the necessity for monitoring of drought conditions in a vulnerable Mediterranean area in order to plan an integrated strategy for climate adaptation. Moreover, the conclusions clarify the usefulness of collaborating innovative very high spatial and spectral resolution EO images along with ground-truth data for crop ET monitoring and also the assimilation into the precision agriculture methodology which is valuable for optimal agricultural production.

Keywords Water availability · Evapotranspiration · Vulnerable agriculture · Remote sensing · Drought · Precision farming

✉ Emmanouil Psomiadis
mpsomiadis@gmail.com

¹ Department of Civil Engineering, University of Thessaly, Volos, Greece

² Department of Natural Resources Management and Agricultural Engineering, Agricultural University of Athens, Athens, Greece

³ SIGMA Geotechnologie, Munich, Germany

1 Introduction

Food production availability is directly affected by climate change worldwide (Hansen 2002; Sultan and Gaetani 2016). The variability and change of seasonal precipitation patterns, evaporation, soil moisture storage and runoff is a significant impact of climate change (Dalezios 2011; Climate Policy Watcher 2017). Temperature and precipitation alteration and the increasing frequency and severity of environmental hazards are directly influenced by climate alterations (Dalezios et al. 2017). The Mediterranean basin is characterized by vulnerable agriculture, because of the combination of temperature increase and precipitation decrease (Dalezios et al. 2018). Food supply can be at increasing risk as yield variability increases (Ahmed and Nithya 2016). In extreme weather events, raise of the yield variability and decrease of the average yield are expected (Alexandrov and Hoogenboom 2000).

Crop water availability and requirements become a significant factor in vulnerable agriculture and drought-prone agricultural areas. There are several commonly used Drought Indices (DIs) based on conventional (ground) and earth observation data (Heim 2002; Niemeyer 2008; Kanellou et al. 2008). Traditional drought assessment methods depend on typical hydrometeorological data, which usually are limited in a region, often unavailable in near real-time and inaccurate (Thenkabail et al. 2004). On the contrary, Earth Observation (EO) data are constantly available and reliable for the detection of drought indicators and characteristics. Moreover, the increasing number and capability of relevant EO satellite systems provide a wide range of innovative abilities, which are suitable to evaluate and monitor drought effects.

WorldView-2 (WV-2) is a commercial Earth observation satellite that provides very high resolution spatial data (VHR-0,5 m). The available imagery introduces four new advanced multispectral bands (especially the yellow, red edge and Near Infrared 2) in addition to the four standard conventional bands (three of the visible spectrum and the common near infrared). These novel spectral bands of potential importance increased significantly the spectral information, which, along with the very high spatial resolution of WV2 imagery, provides the potential for more robust and accurate discrimination between crop types and their characteristics (Salehi et al. 2012; Psomiadis et al. 2017).

Remote Sensing derived Vegetation Indices (VIs) have been broadly utilized to monitor changes in the biophysical properties of plants, such as vegetation cover, vigor, and growth dynamics (Rafn et al. 2008; Mulla 2013; Abuzar et al. 2014). Having as a goal to define vegetation health, distinguish vegetation from soil, estimate evapotranspiration (ET) and water requirements modeling, the calculation of VIs like NDVI constitutes a crucial processing step (Rouse et al. 1974).

Irrigation has always been significant for cultivation yield in most Mediterranean countries, principally because of the high evapotranspiration rates and limited precipitation inputs (Bampzelis et al. 2014). The irrigation water demands are expected to increase in a dry climate, rising the antagonism between water consumers, such as agriculture, urban, and industry (Olesen and Bindi 2002). Precision agriculture composes a recent sophisticated approach with a view to managing the concerns of water availability and needs for efficient crop monitoring in vulnerable agroecosystems (Dalezios et al. 2012b). The increased reliability and accuracy of the EO data lead to better monitoring and analysis, and aims to implement appropriate precise spatiotemporal actions to achieve a low-input, high-efficiency, sustainable agricultural production (Varella et al. 2015).

The present study aims to reveal water availability and requirements in the Mediterranean region's vulnerable agroecosystems based on remote sensing data and methods, and to use

precision agriculture approaches to attain optimal crop water monitoring and irrigation management. A drought-prone area characterized by vulnerable farming is selected, namely Thessaly in central Greece. Water availability is considered through rainfall frequency analysis and drought assessment. Specifically, the remotely sensed Reconnaissance Drought Index (RDI) was used for meteorological drought estimation (Tsakiris and Vangelis 2005; Dalezios et al. 2012a). For the detection of agricultural drought and its impacts, the adjusted Vegetation Health Index (VHI) was utilized (Kogan 2001; Dalezios et al. 2014). Crop water requirements are also assumed within the precision agriculture context by assessing crop evapotranspiration (ET) through the synergistic use of WV-2 satellite images with ground-truth data sets (Psomiadis et al. 2016; Dercas et al. 2017). The satellite-based ET_{csat} is produced by means of the reference ET_o derived from FAO-56 using meteorological data (Allen et al. 1998), and K_c calculated from NDVI making use of the Red and NIR satellite bands.

2 Study Area

The region of Thessaly in central Greece represents approximately 10.6% of the country's territory with an area of 14,036 Km² (Fig. 1), out of which 36% of the area is flat, 17.1% is semi-mountainous, whereas the remaining 44.9% is mountainous. The west part of Thessaly has a continental climate with cold winters, hot and dry summers and large seasonal temperature variations. On the other hand, the east part of Thessaly is described as a typical Mediterranean climate. The mean annual precipitation of Thessaly is approximately 700 mm, with an unevenly spatial and temporal distribution, which varies from about 400 mm at the central plain area to more than 1850 mm at the western mountain parts. The mean annual precipitation at the Thessalic plain, has been reduced about 20% over the last 30 years (Dalezios 2011) and ranges from 250 to 500 mm.

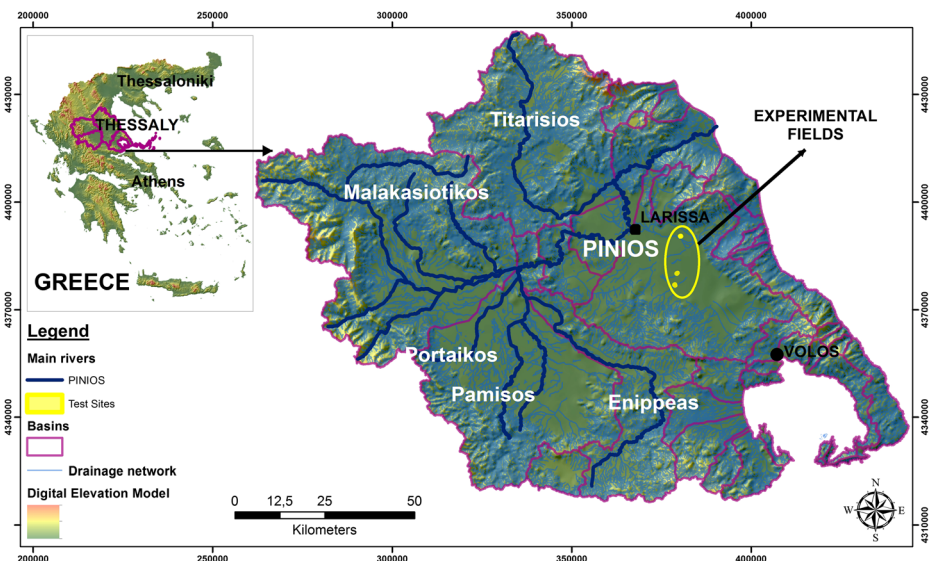


Fig. 1 Geophysical map of Thessaly with the location of the experimental fields

The main crops are cotton, wheat, sugar beets, maize, barley, horticulture, fruits, olive trees and recently energy crops. The 96% of the total water use in Thessaly consumed for irrigation purposes. Extreme hydrometeorological events, such as floods, hail and droughts are common in Thessaly. Droughts occur mainly due to reduced precipitation causing lack of soil moisture, increased evapotranspiration, increased vegetative stress, runoff reduction, decrease in streamflow levels in rivers, lakes and dams, lowering of the groundwater table, and finally water deficit for agriculture.

3 Water Availability

Climate variability and change affect the water availability of the vulnerable agriculture of Thessaly. For this reason the trend of precipitation is analyzed, as well as drought assessment. A brief description of the approaches follows.

Annual precipitation is expected to decrease, causing water shortage in the agricultural sector mainly due to long-duration droughts. Moreover, average yields are anticipated to decrease in the Mediterranean region. Several studies show an increase in drought frequency for almost most parts of Europe, especially in eastern and central part, where there is an increase in the projected irrigation water requirements. A time series of daily precipitation for two separate periods from Larissa meteorological station were utilized to define variability and frequency changes (Dalezios et al. 2009; Bampzelis et al. 2006).

The basic features of drought consist of a lack, or deficit, of precipitation, which justifies the critical role of reliable and long-term precipitation records. Drought monitoring and assessment methodologies rely essentially on rainfall data, which are most of the time limited, often inaccurate and, most importantly, not easily accessible in near-real time (Thenkabail et al. 2004). If the pattern of regional precipitation is typically seasonal, then it is significant to identify the “critical” regional precipitation period(s). The difficulty for some Drought Indices (DIs) may be the lack of a sufficient record length, such as the case of remotely sensed data. Nevertheless, remote sensing data and methods are currently considered a very useful tool for the assessment of the distribution and spatiotemporal features of drought at different scales. It is best to consider multiple indicators to detect and assess the onset and severity of drought.

Drought identification and quantification is not an easy task and it is based usually on indicators and indices. It is clear that there is a necessity for quantification of drought impacts and monitoring of drought development in economically and environmentally sensitive regions. As already mentioned, in order to evaluate and monitor drought, it is essential to detect several drought features, such as severity, duration, onset, end time, areal extent and periodicity. The remote sensing techniques, data and methods allow us to delineate the spatiotemporal variability of several drought features in quantitative terms (Dalezios et al. 2012a, 2014).

3.1 Data Set

For the water availability analysis, the existing daily temperature and precipitation records were utilized from Larissa meteorological station. The data cover an adequate time span of 46 years (1955–2000) which was a period without missing data. The precipitation data were classified into nine classes ranging from light to extreme events, and the number of precipitation events per class was calculated. For the period 1955–1975, the temperature trend is

decreasing, whereas for the period 1976–2000 is increasing (Bampzelis et al. 2006). Therefore, the data were divided into two phases, namely 1955–1975 and 1976–2000. Since the extent of the two periods was different, the precipitation frequencies were normalized.

Daily precipitation data for Thessaly water district (with a spatial resolution of $50 \times 50 \text{ km}^2$) for the Reconnaissance Drought Index (RDI) evaluation were utilized (acquired from the Joint Research Center, Ispra, Italy). The main area is flat with no complex terrain and the interpolation is effective. Initially, monthly crop coefficient maps, using Corine Land Cover dataset of 2000 were created, as well as maps of sunshine day of the study area (for Middle North Latitude- 39.39°). Furthermore, utilizing spectral bands b4 and b5 as well as bands b1 and b2 of NOAA satellite, ten-day Brightness temperature (BT) (for 20 hydrological years, from October 1981 to September 2001) and NDVI images, were calculated, respectively, with a spatial analysis of $8 \times 8 \text{ km}^2$. For the Vegetation Health Index (VHI) estimation, the same procedure was followed.

3.2 Remotely-Sensed Estimation of RDI

For the quantitative assessment of meteorological drought, the remotely sensed RDI was developed and evaluated using a specific methodology, a brief description of which follows (Tsakiris and Vangelis 2005; Tsakiris et al. 2007).

Preprocessing The 10-day NDVI maps of NOAA/AVHRR, are actually the estimated Maximum Value Composite (MVC) images. Likewise, the thermal bands of NOAA were converted firstly to radiance values and then to BT. The concluding preprocessing steps regard the noise removal from the NDVI and BT images and finally the calculation of the final NDVI and BT images, over a monthly time span, by means of MVC and mean pixel values of BT, respectively.

More specifically, as far as it concerns the used filters, a median filter (3×3 to 7×7 window range, depending on each image needs) was implemented to NDVI images, while a conditional mean spatial filter, adjusted only to the pixels that present errors, was applied for BT images smoothing, which appear with a continuous spatial fluctuations (Dalezios et al. 2014).

Calculation of Air Temperature Land Surface Temperature (LST) is estimated by means of NDVI and BT images (Kanellou et al. 2008; Dalezios et al. 2012a). The mathematic formula utilized for the calculation of LST is extracted from the relationship between LST and air temperature (T_{air}) and is given by Eq. (1):

$$T_{air} = 0.6143 * LST + 7.3674 \dots \dots R^2 \approx 0.82 \quad (1)$$

Air temperature maps were calculated from the LST images and ground measurements of air temperature derived from Larissa meteorological station, utilizing regression analysis (number of observations = 500, standard error = 0,4).

Estimation of Potential Evapotranspiration (PET) PET was calculated using the Blaney-Criddle (1950) method that is appropriate for areas with dry and hot summers such as the Mediterranean region, instead of Thornthwaite method, which is more suitable for type of weather with wet and hot summers (e.g., East U.S.A). The RDI is estimated by means of

precipitation and PET. Blaney and Criddle (1950) evaluated the monthly potential evapotranspiration (ET_m) in mm, by the Eq. (2):

$$ET_m = k*[0.46T + 8.16]*p \quad (2)$$

where T is the mean monthly air temperature, p is the monthly daytime sunshine duration, depending on the latitude, and k is the crop coefficient.

The mean monthly crop coefficients, as well as maps of daytime sunshine duration (p) were calculated in a Geographical Information System. These final maps were combined with the corresponding air temperature maps, to extract the Blaney-Criddle PET for each month (in the selected time series, from 1981 to 2001).

Extraction of Rain Map RDI estimation requires the computation of monthly areal precipitation. In this study, monthly rain maps over Thessaly were provided by JRC, ISPRA, from 1975 to 2005 with a spatial resolution of $50 \times 50 \text{ km}^2$. Specifically, from daily rainfall time series, the monthly cumulative rain for each hydrological year was calculated. Linear interpolation method was used for the produce of the montly rain maps.

Remotely-Sensed Assessment of RDI RDI estimation uses monthly temperature maps, crop coefficient (K_c) maps, sunlight maps (p), PET maps based on Blaney- Criddle (1950) and rain maps (P). In the present study, RDI was estimated on monthly and annual basis. The estimation of RDI has been described in the original publication (Tsakiris et al. 2007) and uses the following equation:

$$a_k = \frac{\sum_{j=1}^{j=k} P_j}{\sum_{j=1}^{j=k} PET_j} \quad (3)$$

where P_j and PET_j refer to the precipitation and potential evapotranspiration, correspondingly, of the j -th month of the hydrological year. In the Mediterranean region, the hydrological year starts in October, hence for October $k=1$. RDI_n is the Normalised RDI, which is given by Eq. (4):

$$RDI_n(k) = \frac{a_k}{\bar{a}_k} - 1 \quad (4)$$

The Standardised RDI (RDI_{st}), is used.

$$RDI_{st}(k) = \frac{y_k - \bar{y}_k}{\hat{\sigma}_k} \quad (5)$$

where y_k is the $\ln a_k$, \bar{y}_k is its arithmetic mean and $\hat{\sigma}_k$ is its standard deviation. The drought categories based on RDI are shown in Table 1.

3.3 Remotely Sensed Estimation of VHI

VHI is a very accurate and widely used index and was applied for the quantification of agricultural drought. VHI estimation utilizing earth observation data follows a certain

Table 1 RDI drought classification scheme (Tsakiris and Vangelis 2005)

Drought classes	RDI Values
Extremely wet	>2.00
Very wet	1.50 to 1.99
Moderately wet	1.00 to 1.49
Near normal	-0.99 to 0.99
Moderately dry	-1.00 to -1.49
Severely dry	-1.50 to -1.99
Extremely dry	< -2.00

methodology (Dalezios et al. 2014). A preprocessing phase, which includes geometric and atmospheric correction of all images, was implemented. Subsequently, the VHI was estimated on a pixel basis.

Preprocessing Ten-day EO data from NOAA/AVHRR satellite were used with pixel resolution $8 \times 8 \text{ Km}^2$. Low pass smoothing filters were utilized, analogous to RDI mentioned above. The extracted variables from satellite data are BT and NDVI, respectively, on a monthly time span.

Vegetation Health Index (VHI) The final step comprises the monthly calculation of BT and NDVI, respectively. The VHI is the sum of the Vegetation Condition Index (VCI) and the Temperature Condition Index (TCI), both calculated from the EO data, as described in the original publications (Kogan 1995, 2001). VCI reflects the growth difference of crops among different years and acts as an extension of NDVI (for NDVI_{\max} , VCI is equal to 100) and is computed by the following Eq. (6):

$$\text{VCI} = 100 * \frac{\text{NDVI} - \text{NDVI}_{\min}}{\text{NDVI}_{\max} - \text{NDVI}_{\min}} \quad (6)$$

where NDVI, NDVI_{\max} and NDVI_{\min} correspond to the smoothed 10-day NDVI, its multi-annual minimum and maximum, respectively. Likewise, TCI depends on the same concept as VCI and is calculated by the Eq. (7) (for BT_{\max} , TCI is equal to 0):

$$\text{TCI} = 100 * \frac{\text{BT}_{\max} - \text{BT}}{\text{BT}_{\max} - \text{BT}_{\min}} \quad (7)$$

where BT, BT_{\max} and BT_{\min} correspond to the smoothed 10-day radiant temperature, its multi-annual minimum and maximum, respectively.

The VHI characterizes the total vegetation health and is widely utilized widely for drought monitoring and crop yield valuation.

Agricultural drought is demonstrated by five classes of VHI in Table 2. Unambiguously, from Table 2 it is clear that drought severity is decreasing when VHI values are increasing. VHI is calculated by the Eq. (8):

$$\text{VHI} = 0.5 * (\text{VCI}) + 0.5 * (\text{TCI}) \quad (8)$$

VHI takes values from 0 to 100, where 0 indicates extreme stress and 100 indicates favorable conditions. VCI and TCI depict the moisture and thermal conditions of vegetation, respectively (Kogan 2001). Since moisture and temperature contributions during the

Table 2 VHI drought classification classes (Kogan 2001)

VHI values	Vegetative drought	Classes numbers of drought
VHI < 10	Extreme	1
VHI < 20	Severe	2
VHI < 30	Moderate	3
VHI < 40	Mild	4
VHI > 40	No	–

vegetation cycle were not specified, an equal weight has been hypothesized for both VCI and TCI, in the VHI calculation. Thermal conditions are especially important when moisture shortage is accompanied by high temperature, increasing the severity of agricultural drought and having a direct impact on vegetation health. In many parts of the world, TCI along with VCI have also proven to be useful tools for the detection of agricultural drought (Dalezios et al. 2014; Kogan 2001).

4 Water Requirements

Precision agriculture methodology for the estimation of the water needs requires a combination of field observations, such as crop characteristics and water requirements, along with meteorological data, so as to assess reference evapotranspiration (ET_0). High-resolution satellite images are also utilized to evaluate the variability and spatial distribution of crop coefficient (K_c) and evapotranspiration (ET_c) (Dalezios et al. 2011) and contribute through processing and analysis to decision support at field level (Dalezios et al. 2012b).

4.1 Experimental Fields and High-Resolution EO Data

Three agricultural fields of cotton (1.8 ha, 2.1 ha, 4.3 ha) were used throughout the growing season of 2015, 2016 and 2017 in Thessaly plain area (Fig. 2a). Eleven WV-2 scenes were processed having an exceptional spatial and spectral resolution (0.5 m and eight multispectral bands) (Fig. 2).

Soil water content and meteorological data (rainfall, temperature, wind speed) were monitored during the three growing seasons. Soil moisture sensors (EC-5 and 10HS sensors of Decagon Devices, Inc.) were installed in every experimental field. The sensors were placed to a depth of 30 cm as representative of the whole root zone and readings were taken regularly with a portable device. At farm level there were also continuous moisture profile measurements, taken every 2 h at 4 or 5 depth levels spanning from 15 to 90 cm with EM50 data loggers in order to monitor the whole profile of soil moisture in a single position or two positions of the fields. Using the soil moisture data at 30 cm depth, we charted the spatial distribution of the whole farms. The soil moisture data allowed us to evaluate the water conditions in the root zone and to estimate if the crops suffer from any water stress.

Image Preprocessing and Rectification The relationship between the radiance of the electromagnetic radiation reflected by ground targets and that measured by the satellite instrument

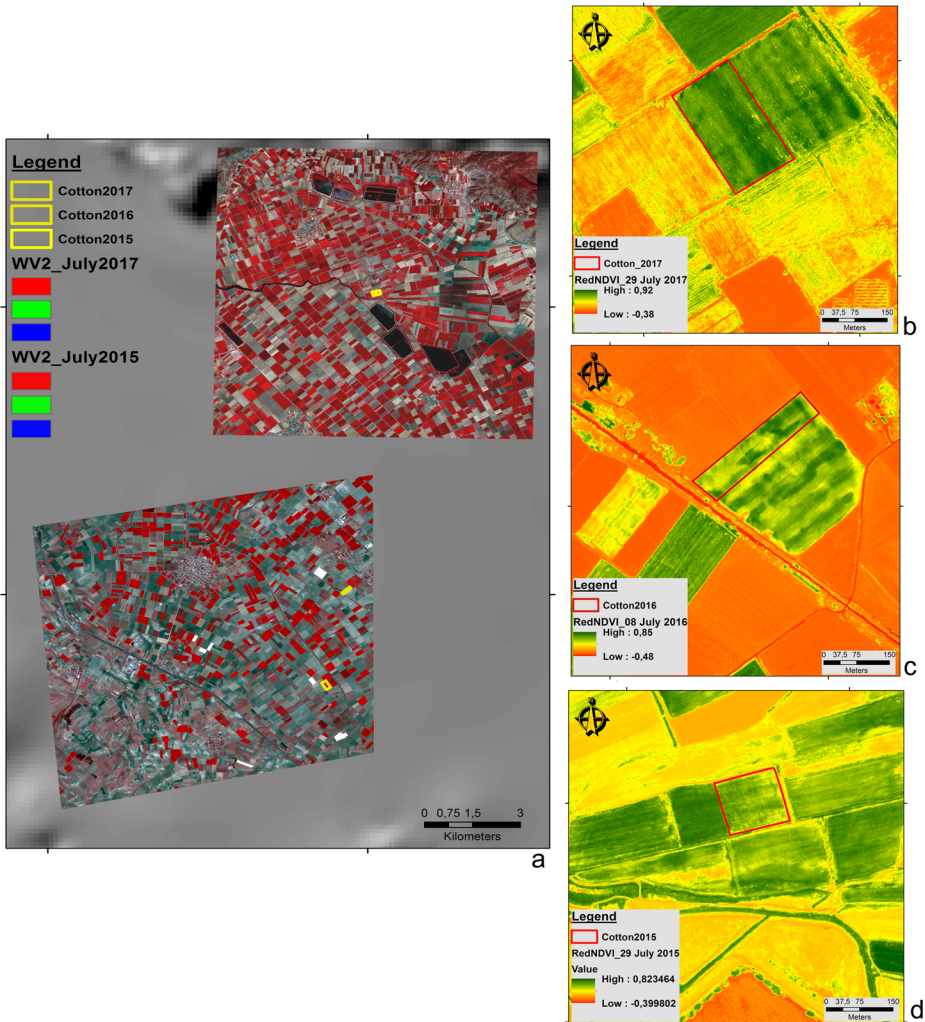


Fig. 2 a The shape and area of the three experimental fields, b, c, d The redNDVI extracted from the three selected cotton crops

is a complex one. The radiance emitted at ground level passes through the intervening atmosphere (clouds, vapor, aerosol and haze) on its way to the satellite while there are also possibly geometrical distortions by imperfection in the sensor optical components and by the effects of varying ground terrain. Overall there is a major requirement for calibration, preprocessing, correction and rectification of imagery before it can be used in any qualitative or quantitative analysis.

Three WV-2 series of scenes from May, June, July and September of 2015 (4 images), from July and Aug 2016 (2 images) and from May, June, July, August and September 2017 (5 images) over cotton fields were atmospherically corrected, radiometrically enhanced and georeferenced (Lanzl and Richter 1991; Updike and Comp 2010). Four WV2 for the cotton farm of 2015 and seven scenes for the cotton farms of 2016 and 2017 were used, respectively. The local different weather conditions occurred during the acquisition of the

cloud free imagery, seasonal atmospheric models for the concerned geographic latitude, the type of land-use and 5 m Digital Elevation Model were used to run the corrections of the data. Initially a top of the atmosphere reflectance image (ToA) was created to be followed by haze removal and cloud masking process, converting Digital Numbers (DN) to reflectance values above the atmosphere. Reflectance values were then transformed to ground reflectance taking into account the solar azimuth and zenith angles on the acquisition date (Lanzl and Richter 1991; Dercas et al. 2017). The ATCOR3 Top of the Atmosphere and Ground reflectance workflows available in Geomatica 2016 system were used. ATCOR has already available the WV2 sensor gain and offset parameters (mW/cm² sr micron). The subsequent geometric correction followed two different geocoding approaches, by means of image-to-GCPs and image-to-image registration. The first acquired image for the three cotton fields was used as master to slave all the rest. The first WV-2 acquired on May 17, 2015 and corrected using 10 GCPs, acquired from a differential GPS, while all the other images were registered using as reference for the first image. It has to be mentioned that the area of the cotton fields is relatively flat with no terrain fluctuations and the farm sizes is not more than 5 ha. The bilinear algorithm was used to correct the sensor optical aberration satellite instabilities and terrain variations. This algorithm does not alter the DN values of the pixels, a critical decision for the subsequent qualitative analysis and build of vegetation indices. In all cases a half pixel RMR error was achieved in X and Y axes.

Image Processing Initially, three different band combinations or False Color Composites (FCCs), of pan-sharpened fusion data were processed and developed to assist the subsequent field interpretation work. Pan-sharpening is the result derived from the fusion of 2 m multispectral channels with the 0.5 m panchromatic band to generate multispectral bands that maintain the spectral information, but in higher spatial resolution of 0.5 m, thus enhancing the information analysis and clarity, which is very important for the fragmented small mixed and multiple land-uses of Mediterranean agricultural fields. The first FCC was the 5,3,2 (red, green, blue) using the visible part of the electromagnetic spectrum. The second was the 6,5,3 (redEdge, red and green) and the third one the 8,5,4 (NIR2, red and yellow). The two latter combinations exhibited and depicted crop and soil variations (Fig. 3).

The reflectance calibrated WV2 data then processed to build the VIs such as Chlorophyll, redNDVI and redEdgeNDVI using red, redEdge and the two near infrared channels NIR1 and NIR2. The use of the second innovative near-infrared band of WV2 is the first attempt to reach better quality VIs, since is less influenced by the atmosphere.

In Mediterranean agricultural areas, the NDVI derived from very high spatial analysis WV2 data has shown that it constitutes a significant indicator of green biomass vegetation density and health. NDVI uses leaves chlorophyll properties that demonstrates high energy absorption in the RED part and high reflectance in the Near-Infrared (NIR) part of electromagnetic spectrum, and uses the following formula (Eq. 9):

$$\text{NDVI} = (R_{\text{NIR}} - R_{\text{RED}}) / (R_{\text{NIR}} + R_{\text{RED}}) \quad (9)$$

where R is the reflectance. The NDVI takes pixel values from -1 to 1. In general NDVI lower than 0.2 correspond to non-vegetated surfaces, while NDVI greater to 0.2 to vegetated ones. (Figs. 2, 3 and 4).

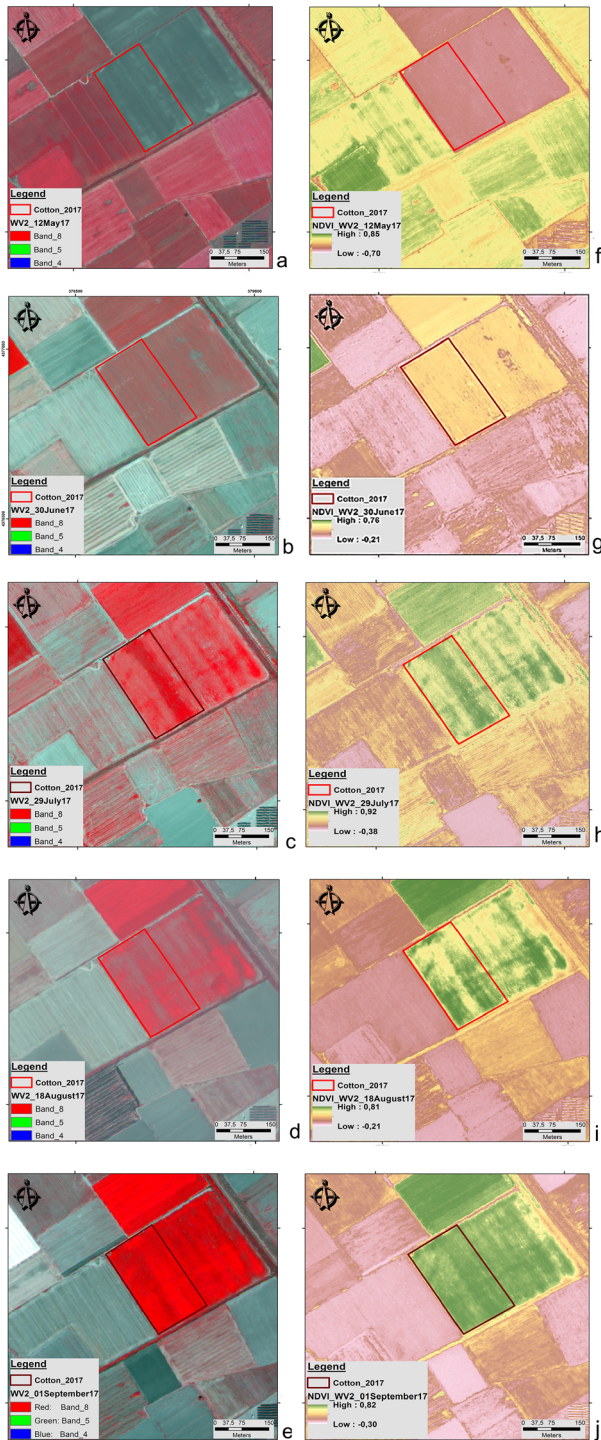


Fig. 3 a–e WV-2 False Color Composites (using NIR2 band – 8,5,4-RGB) of May, June, July, August and September 2017, f–j The cotton crop redNDVI of 2017, for the 5 months, respectively

The redEdge NDVI index $(nir-redEdge)/(nir+redEdge)$ had different behavior from NDVI. WV-2 red edge channel is more sensitive to the change of vegetation reflectance so it was also generated to monitor cotton phenological cycle. Additionally, Chlorophyll index $[(nir/redEdge)-1]$ was also produced to extract and monitor the behavior of local cotton farm.

In conjunction with meteorological and ground data, as well as models, the imagery was utilized to calculate reflectance, NDVI, fractional cover, crop coefficient (K_c) and crop evapotranspiration (ET_c) maps over the image coverage.

Estimation of ET_0 Reference evapotranspiration (ET_0) is calculated by the Penman-Monteith method created according to FAO-56 using conventional meteorological data and it is reliable with the water use data of the crops (Allen et al. 1998) (Eq. 10):

$$ET_0 = \frac{0.408(R_n - G)\Delta + \gamma \left(\frac{900}{T_{mean} + 273} \right) u_2 (e_s - e_a)}{\Delta + \gamma(1 + 0.34u_2)} \quad (10)$$

where: T_{mean} is mean temperature ($^{\circ}C$) and u_2 is 2 m height wind speed.

Estimation of K_c The crop coefficient (K_c) is developed from NDVI index using red, NIR1 and NIR2 channels of WV-2. The K_c integrates the effect of features that distinguish a typical crop cultivation from the reference type of grass reference, having a uniform and a completely ground cover appearance. The K_c values depend on crop type and growth stages, climate and soil evaporation (Allen et al. 1998). In FATIMA project, the following relationship was developed as follows (Dercas et al. 2017) (Eq. 11, number of observations = 1.000, standard error = 0,12):

$$K_c = 1.33^* (redNDVI) + 0.21 \quad (R^2 = 0.92) \quad (11)$$

Estimation of Crop Evapotranspiration ET_c Crop Evapotranspiration ET_c is the evapotranspiration from a crop with good health, optimum conditions of irrigation, fertilization, growing in large fields, and achieving high production yields under specified climatic conditions (Allen et al. 1998). In FAO method, ET_c is calculated as follows (Eq. 12):

$$ET_c = K_c * ET_0 \quad (12)$$

where ET_0 is calculated by ground-based observations. The satellite-based ET_{csat} is calculated by utilizing the reference ET_0 from FAO-56 Penman-Monteith formula derived from meteorological data (Allen et al. 1998) and K_c extracted using redNDVI of WV-2, respectively. If a complete data set is not available for the usage of Penman-Monteith equation, several other empirical equations could be operative, such as Hargreaves or Turk models, among others. In this analysis due to reduced meteorological data crop Evapotranspiration (ET_c) was estimated with Hargreaves equation, using FAO crop coefficients. Actual evapotranspiration was adjusted with ground moisture measurements and according to the water balance method at the farm level.

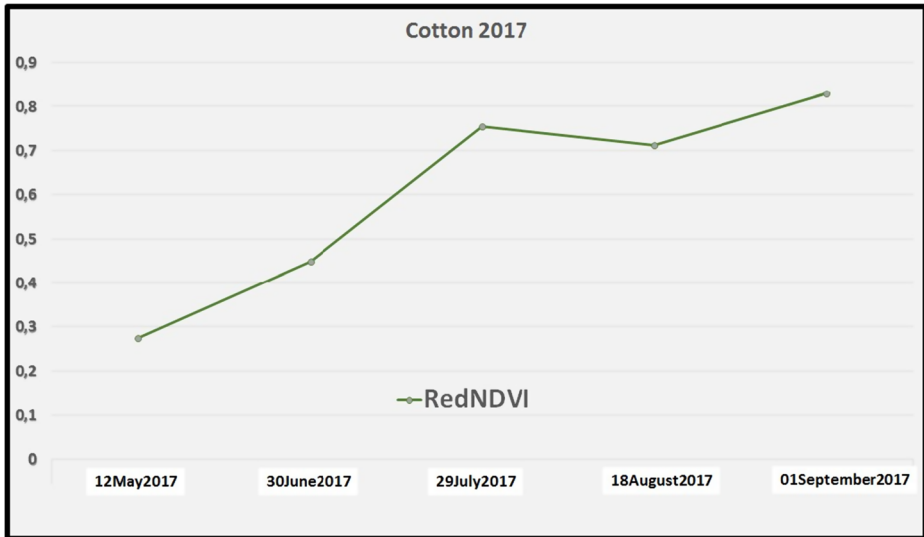


Fig. 4 Cotton 2017 redNDVI variation along the cultivation period

5 Results and Discussion

5.1 Analysis of Results

The results of the precipitation frequency demonstrate that in Thessaly there were indications of a shift towards higher precipitation intensities for the period after 1975 (Dalezios et al. 2009). More specifically, precipitation of a slightly greater volume but less frequent was recorded in the Larissa station for the period 1955–1975 as related to the latest period (1976–2000) (Fig. 5). This element reveals a trend for precipitation events with smaller total amounts, but of increased intensity that causes floods and greater loss of water. The reduction of precipitation inputs and decrease of water availability could adversely affect future crop production in the region and consequently the local economy.

The results of RDI analysis are summarized in Fig. 6 and Table 3. Specifically, Fig. 6 is a plot of the computed RDI annual time series for Larisa, where the negative RDI values represent drought years and the positive RDI values refer to non-drought years based on the RDI classification scheme of Table 1.

In Fig. 6, the term conventional RDI means computation of the RDI from conventional meteorological data at Larisa station, whereas satellite RDI means the corresponding remotely sensed RDI values, as computed for a 3×3 pixel area above the Larisa station.

The results of Fig. 6 indicate that there were eight drought episodes during this 20-year period in the study area of Thessaly, Greece. Moreover, the duration, as well as the start and end times of droughts of Fig. 6 based on RDI monthly estimates, coincide with the duration and start of the hydrological year in most of the cases, i.e., 12 or 13 months in duration starting in October. The RDI time series of Fig. 6 constitutes the basis for frequency and/or periodicity

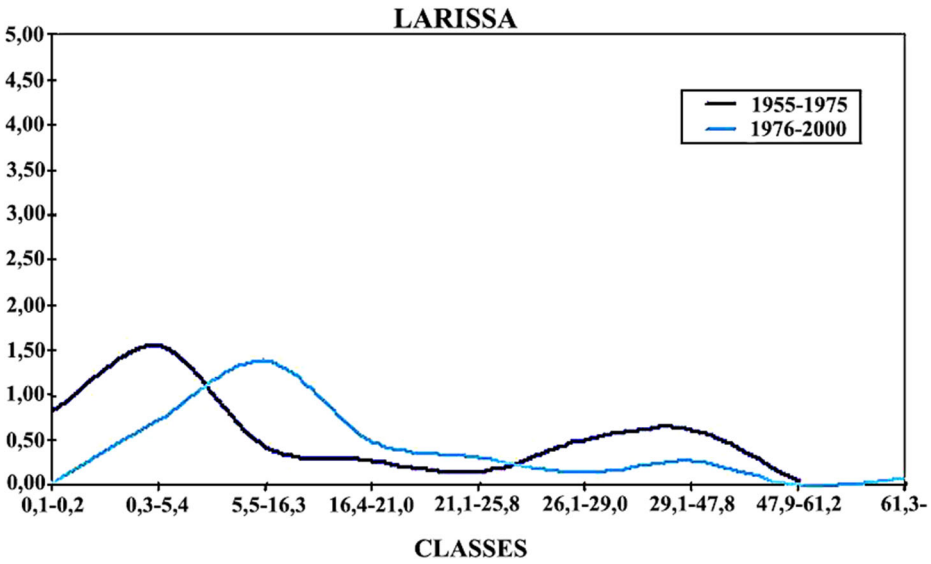


Fig. 5 Precipitation Frequency analysis for Larissa station (from Dalezios 2011)

analysis (Dalezios et al. 2000). Table 3 demonstrates in pixels the monthly areal distribution of the RDI values, which sums the four severity classes of drought for each of the eight drought hydrological years. From Table 3 it is assessed that in Thessaly during the drought years, two classes of droughts were revealed, high and low severity, respectively, based on the cumulative areal extent.

Moreover, several additional findings can be extracted by comparing Fig. 6 and Table 3. In particular, it can be specified that drought usually starts during the first 3 months of the hydrological year as far as it concerns the years of considerable areal extent, whereas drought begins in spring (April or May) in the years of small areal extent.

The monthly results of VHI for the same period of 20 years (1981–2001) using satellite data are presented in Table 4 (for high drought severity classes 1 and 2) and Table 5 (for low

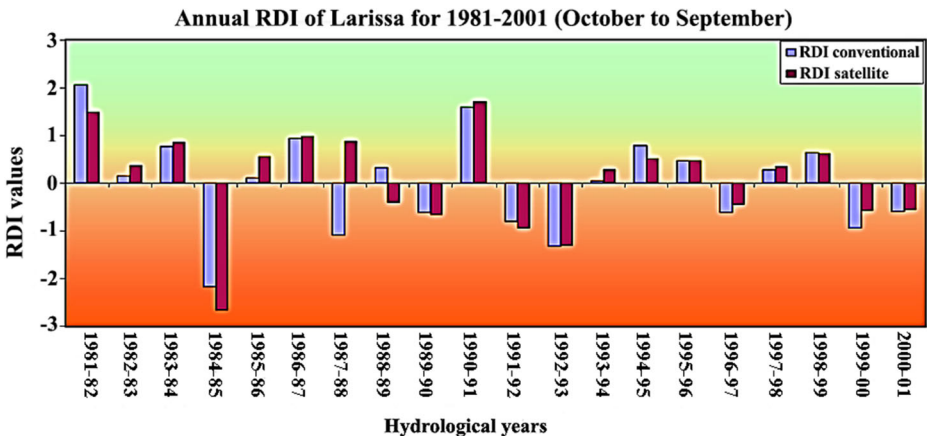


Fig. 6 Annual RDI of Larissa for 1981–2001 (October to September, from Dalezios et al. 2012a)

Table 3 Drought years' monthly areal extent (period 1981–2001), in number of pixels (pixel size 8×8 km) (from Dalezios et al. 2012a)

Year Month	1984–85	1987–88	1989–90	1991–92	1992–93	1996–97	1999–00	2000–01
October	207.70	0.04	75.21	81.91	111.18	2.59	25.98	16.68
November	84.98	0.23	167.91	163.81	128.34	207.77	8.40	207.69
December	95.53	66.21	23.02	205.77	203.18	45.35	74.16	205.27
January	82.09	86.31	207.71	207.65	199.04	72.43	199.30	40.96
February	2.44	0.24	207.79	207.496	45.35	199.36	22.15	164.46
March	0.27	0.22	207.79	203.925	199.72	201.37	207.42	207.61
April	167.15	127.71	159.59	0.22	206.44	0.41	203.73	4.85
May	125.92	196.15	2.09	12.47	0.11	207.76	185.27	14.04
June	205.14	59.79	161.48	8.48	114.88	16.73	12.29	133.98
July	128.74	60.47	40.13	8.39	201.54	146.55	171.26	0.09
August	114.99	130.75	0.25	203.84	191.96	0.13	193.57	49.07
September	123.33	83.68	77.02	204.07	81.29	203.82	75.57	199.30
Total	1338.27	811.80	1330.01	1508.02	1683.01	1304.26	1379.09	1244.01

drought severity classes 3 and 4), respectively, based on the VHI classification scheme of Table 2. In particular, extreme and severe drought classes 1 and 2 merged into one class (Table 4), and moderate and mild drought classes 3 and 4 merged into a second class (Table 5), respectively. The analysis of agricultural drought based on VHI estimation shows that drought takes place every year from April till October, during the warm period. Moreover, Tables 4 and 5 display the monthly total and the average for the merged classes, where the greater number of pixels is gathered among mild and moderate drought severity classes (Table 5). On the other hand, according to Table 4, the number of pixels of monthly extreme drought classes is relatively small. Additionally, Tables 4 and 5 reveal that the peaks of drought severity and areal extent appear mainly at the end of the summer period.

In summary, eight drought periods enduring 12 months each in a 20-year study period were detected, for meteorological drought based on RDI. Nevertheless, during the warm season (from April to October) agricultural drought is appeared to occur every year, utilizing the VHI approach. The above mentioned findings rationalize the new scientific trend to develop and create composite drought indices for regional drought evaluation and monitoring (Dalezios et al. 2017).

The results of water requirements are summarized in Fig. 7, and Tables 6 and 7. The estimated K_{csat} (K_c assessed using satellite data) average values for cotton at the field scale are computed from Eq. (11) and the K_c from FAO for cotton during the growing season of 2015.

The cotton K_{csat} values based on Red and NIR spectral bands of WV-2 data are quite similar to the K_c values from FAO for 2015, (Fig. 7). Indeed, K_{csat} is dependent on the type of satellite data and cannot be implemented in a generic way. Spatial and spectral resolutions are the critical components of any sensor, which is used for K_{csat} extraction. Additionally, the type and size of fields, such as small size farms or land fragmentation, plays a role on the satellite data and thus on the K_c equation to be used. The K_c obtained by the new proposed Eq. (11) (using the NDVI obtained by WV-2 images) for 2015, 2016 and 2017 are presented in Table 6. In Table 7 the ET_c estimated according to K_{cFAO} and K_{csat} are presented. In both cases the ET_0 was estimated using the Hargreaves method due to limited meteorological data. The values of ET_{csat} and ET_{cFAO} are in good agreement for both methods, which is a promising mark for the new WV-2 approach. The water conditions in the experimental fields were

Table 4 Monthly drought VHI values and their cumulative areal extent (number of pixels) (calculation of severity classes 1 and 2) (from Dalezios et al. 2014)

Cummulative							
	May	June	July	August	September	October	SUM
1981	0	0	19	38	65	66	188
1982	0	1	14	28	31	31	105
1983	0	9	10	13	17	17	66
1984	0	1	6	10	10	10	37
1985	0	12	30	58	71	71	242
1986	0	3	13	25	33	33	107
1987	0	0	7	8	17	17	49
1988	0	10	24	36	40	40	150
1989	1	19	36	43	53	53	205
1990	3	39	57	69	69	69	306
1991	0	0	1	2	2	2	7
1992	0	2	3	5	5	5	20
1993	0	1	2	10	10	10	33
1994	0	0	0	0	0	0	0
1995	0	0	17	20	20	20	77
1996	1	13	18	19	19	19	89
1997	0	0	2	2	3	3	10
1998	0	2	3	11	12	12	40
1999	0	6	6	7	7	7	33
2000	1	2	12	17	18	18	68
2001	0	7	15	15	15	0	52
	6	127	295	436	517	503	
Average	0.29	6.05	14.05	20.76	24.62	23.95	
SD	0.72	9.27	13.84	18.68	22.45	23.09	
Min	0	0	0	0	0	0	
Max	3	39	57	69	71	71	

analyzed for all the cases and were not under any water stress. The actual evapotranspiration was estimated and showed that the crops were well irrigated. This was an essential condition in order to be able to confirm that the Kc evaluated was not a Kc stress.

5.2 Discussion

The ambition of this research effort has been to increase the water use efficiency by better matching spatiotemporal supply with crop demand. In order to achieve the above goal, new incentives and policies for ensuring the sustainability of agriculture and ecosystem services are needed in addition to new technology and methods.

Precision agriculture is certainly considered a high-technology advanced approach to agriculture. The main interest remains on the implications of high technology for agriculture. At the present time, the generally accepted rationale of precision agriculture is that with existing technology, it is possible to match inputs and management at a sub-field scale in a site-specific manner without sacrificing mechanization efficiency. For the farmer, this means to gain the productive benefit of large field mechanized crop production and husbandry on a much smaller scale. By skipping the concept of high technology and costly equipment, the rationale becomes to use as much information as possible in a consistent and controlled manner to achieve the most efficient management of the farm at

Table 5 Monthly drought VHI values and their cumulative areal extent (number of pixels) (calculation of severity classes 3 and 4) (from Dalezios et al. 2014)

Cummulative							
	May	June	July	August	September	October	SUM
1981	0	0	123	252	343	418	1136
1982	8	74	193	321	416	431	1443
1983	36	142	228	331	433	464	1634
1984	6	72	173	266	308	332	1157
1985	23	134	240	361	494	568	1820
1986	45	139	249	350	471	513	1767
1987	9	71	204	287	405	418	1394
1988	19	108	243	359	467	541	1737
1989	18	107	211	315	408	474	1533
1990	84	169	298	422	511	561	2045
1991	0	38	129	203	266	306	942
1992	16	103	174	265	323	374	1255
1993	12	94	173	260	310	352	1201
1994	9	60	101	154	213	236	773
1995	4	44	146	215	278	318	1005
1996	49	148	237	309	338	347	1428
1997	27	124	228	291	358	379	1407
1998	25	106	196	284	336	365	1312
1999	40	145	227	305	357	376	1450
2000	43	129	243	337	421	431	1604
2001	45	141	229	299	345		1059
	518	2148	4245	6186	7801	8204	
Average	24.67	102.29	202.14	294.57	371.48	410.2	
SD	20.88	43.36	48.86	59.92	78.61	89.43	
Min	0	0	101	154	213	236	
Max	84	169	298	422	511	568	

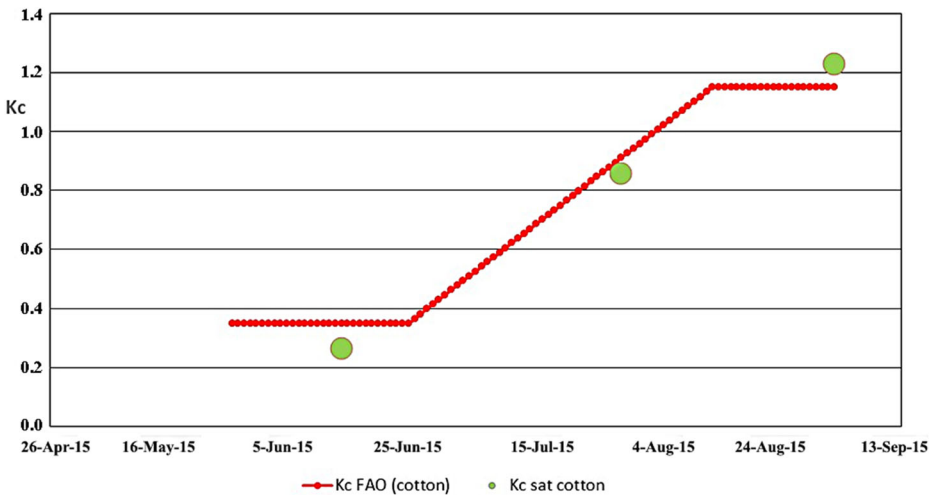


Fig. 7 Comparison of Kcsat from WV-2 and Kc produced by FAO for the cotton field in 2015 (from Dercas et al. 2017)

Table 6 Kc_{FAO} and Kc_{sat} for the WV-2 acquisition days

Cotton 2015			Cotton 2016			Cotton 2017		
Acquisition date	Kc _{FAO}	Kc _{sat}	Acquisition date	Kc _{FAO}	Kc _{sat}	Acquisition date	Kc _{FAO}	Kc _{sat}
						May 12	0,35	0,57
June 13	0,35	0,35				June 30	1,07	0,80
July 29	0,99	0,91	July 8	1,13	0,99	July 29	1,15	1,21
			August 12	1,15	1,05	August 18	1,15	1,16
Sept 2	1,15	1,28				Sept. 1	1,11	1,31

appropriate scales. More specifically, the goals of precision agriculture can be defined as: optimum production and economic efficiency, minimization of risk, limit the impact of agriculture on the wider environment. The implemented Earth Observation (EO) methodology in this research effort for mapping irrigated and rainfed areas and for calculating crop water requirements is considered internationally mature (Calera et al. 2017; Dalezios et al. 2017).

The step forward in this paper, has been to use time series of high and very high spatial resolution images of WV-2 at resolution 0.5 m, to describe, map and assess water stress. Timely and easy-to-use maps about water requirements are the natural way in which the information is valuable for precision farming application.

The results of this paper justify the usefulness of precision agriculture, which, in return, suggests that policies should be analyzed and considered for synergies, conflicts, bottlenecks and set procedures leading to an enabling environment of sustainable crop production. Farm advisers should play a critical role in informing farmers on precision farming tools and methods. This requires the development of specific data analysis tools with special emphasis on cost-benefits. In addition, the potential economic benefits of precision farming are not yet easily measurable and stakeholders often lack the tools to calculate potential profits and benefits. This is partly due to unclear business models of precision farming methods and associated costs and benefits. Furthermore, validated precision farming decision-support models and analytical tools need to be available for farm advisers and farmers. Precision farming can also be useful for small and medium-sized farms, provided that ways are found to reduce investment needs and risk. Finally, more applied research, involving farmers, advisers and supply chain partners, is needed, which is gradually promoted. Relevant research should adopt a systems approach covering social, economic, environmental and technical aspects.

Table 7 ETC_{FAO} and ETC_{sat} for the WV-2 acquisition days (2015, 2016, 2017)

Cotton 2015			Cotton 2016			Cotton 2017		
Acquisition date	ETC _{FAO} (mm)	ETC _{sat} (mm)	Acquisition date	ETC _{FAO} (mm)	ETC _{sat} (mm)	Acquisition date	ETC _{FAO} (mm)	ETC _{sat} (mm)
						May 12	1,96	3,19
June 13	2,42	2,42				June 30	9,46	7,07
July 29	6,65	6,11	July 8	6,24	5,46	July 29	7,19	7,56
			August 12	5,66	5,17	August 18	6,06	6,11
Sept 2	6,64	7,39				Sept. 1	5,35	6,31

6 Summary and Conclusions

Climatic projections indicate decreases in precipitation and increases in temperature, combined with drought events, in the Mediterranean region. Agriculture is estimated to be the most influenced by the adverse impacts of climate change and variability, with a high probability of crop production reductions, due to less lack of irrigation water. The results of the frequency analysis show that there was a shift towards higher precipitation intensities for the second period (after 1975) indicating a trend for precipitation episodes with less amounts, but of increased intensity causing floods and more significant loss of water. Furthermore, trying to decrease the risk of climate change impacts on agriculture, integrated methodologies need to be developed, composing the results of studies on drought and evapotranspiration calculation and monitoring, for the formulation of cost-effective mitigation measures and adaptation strategies. The study outcomes the designation that agricultural drought takes place every year at the warm period with increasing severity and areal extent, having its maximum appearance at the end of summer of summer, which is quite typical in the Mediterranean region. The greater number of pixels is gathered between mild to moderate drought severity classes indicating a significant decrease in the number of pixels from gentle to extreme drought classes for all the months. There is, thus, a new scientific trend of developing composite drought indices for regional drought assessment and monitoring.

The comparison of WV-2 earth observation data with measurements in situ has revealed that the utilization of very high resolution satellite data can definitely be an advantageous tool for precision or operational farming, providing apart from the extraction of crop area a number of valuable parameters, such as ET_c from K_c , that can be utilized for the assessment of crop water needs. The results of the implemented methodology explain the synergistic use of WV-2 images with ground-truth data set for monitoring ET_c in different crops.

Acknowledgements A previous shorter version of the paper has been presented in the 10th World Congress of EWRA “Panta Rei” Athens, Greece, July 2017. The meteorological data were acquired by the Hellenic National Meteorological Service. Earth Observation data were provided by NASA. Research was funded by the INTERREG IIIb PRODIM project, EU FP6 PLEIADES project and by HORIZON2020 FATIMA project. The authors would like to thank the editor and the reviewers for their constructive comments and valuable suggestions.

Compliance with Ethical Standards

Conflict of Interest None.

Publisher’s Note Springer Nature remains neutral with regard to jurisdictional claims in published maps and institutional affiliations.

References

- Abuzar M, Sheffield K, Whitfield D, O’Connell M, McAllister A (2014) Comparing inter-sensor NDVI for the analysis of horticulture crops in South-Eastern Australia. *American Journal of Remote Sensing* 2(1):1–9
- Ahmed A, Nithya R (2016) Within-season growth and spectral reflectance of cotton and their relation to lint yield. *Crop Sci* 56:2688–2701. <https://doi.org/10.2135/cropsci2015.05.0296>

- Alexandrov VA, Hoogenboom G (2000) The impact of climate variability and change on crop yield in Bulgaria. *Agric For Meteorol* 104:315–327
- Allen RG, Pereira LS, Raes D, Smith M (1998) Crop evapotranspiration: guidelines for computing crop requirements. Irrigation and drainage paper no. 56. FAO, Rome, p 300
- Bampzelis D, Chatziplli A, Dadali O, Dalezios NR (2006) Frequency analysis of precipitation characteristics in different climate zones for Greece. In: Proceedings of the 3rd HAICTA international conference: information systems in sustainable agriculture, agroenvironment and food technology, Volos Greece, pp 887–895
- Bampzelis D, Pytharoulis I, Tegoulas I, Zanis P, Karacostas T (2014) Rainfall characteristics and drought conditions interconnected to the potentiality and applicability of the “DAPHNE” rain enhancement project in Thessaly. Conference Proceedings, 10th International Congress of the Hellenic Geographical Society, Thessaloniki, Greece, pp 1–9
- Blaney HF, Criddle WD (1950) Determining water requirements in irrigated areas from climatological and irrigation data. USDA Soil Conservation Service Technical Paper, 96, pp 48
- Climate Change Watcher (2017) <https://watchers.news/category/climate-change/>
- Dalezios NR (2011) Climatic change and agriculture: impacts-mitigation-adaptation. *Scientific Journal of GEOTEE* 27:13–28
- Dalezios NR, Loukas A, Vasiliades L, Liakopoulos H (2000) Severity-duration-frequency analysis of droughts and wet periods in Greece. *Hydrol Sci J* 45(5):751–769
- Dalezios NR, Gkagkas Z, Domenikiotis C, Kanellou E, Mplanta A (2009) Climate change and water for agriculture: impacts-mitigation-adaptation. Proceedings, EWRA conference on water resources conservancy and risk reduction under climatic instability, Techn. Univ. of Cyprus (TUC), sponsored by EWRA and TUC, Limassol, Cyprus
- Dalezios NR, Mplanta A, Domenikiotis C (2011) Remotely sensed cotton evapotranspiration for irrigation water management in vulnerable agriculture of central Greece. *J of Information Technology Agriculture* 4(1):1–14
- Dalezios NR, Mplanta A, Spyropoulos NV (2012a) Assessment of remotely sensed drought features in vulnerable agriculture. *NHESS* 12:3139–3150
- Dalezios NR, Spyropoulos NV, Mplanta A, Stamatiades S (2012b) Agrometeorological remote sensing of high resolution for decision support in precision agriculture. 11th international conference on meteorology, climatology and atmospheric physics. Athens, pp 51–56
- Dalezios NR, Mplanta A, Spyropoulos NV, Tarquis AM (2014) Risk identification of agricultural drought in sustainable agroecosystems. *NHESS* 14:2435–2448
- Dalezios NR, Dercas N, Spyropoulos NV, Psomiadis E (2017) Water availability and requirement for precision agriculture in vulnerable agroecosystems. Proc. EWRA2017, NTUA, Athens Greece, pp 1715–1722
- Dalezios NR, Dercas N, Eslamian S (2018) Water scarcity management: part 2: satellite-based composite drought analysis. *IJGEI* 17(2/3):267–295
- Dercas N, Spyropoulos NV, Dalezios NR, Psomiadis E, Stepopoulou A, Madonakis G, Tserlikakis N (2017) Cotton evapotranspiration using very high spatial resolution WV-2 satellite data and ground measurements for precision agriculture. *WIT Trans Ecol Environ* 220:101–107. *Water Resources Management* 2017, WIT press. <https://doi.org/10.2495/WRM170101>
- Hansen JW (2002) Realizing the potential benefits of climate prediction to agriculture: issues, approaches, challenges. *Agric Syst* 74:309–330. [https://doi.org/10.1016/S0308-521X\(02\)00043-4](https://doi.org/10.1016/S0308-521X(02)00043-4)
- Heim RR (2002) A review of twentieth-century drought indices used in the United States. *Bull Am Meteorol Soc* 83(8):1149–1165
- Kanellou E, Domenikiotis C, Dalezios NR (2008) Description of conventional and satellite drought indices. In: Tsakiris G (ed) Proactive management of water systems to face drought and water scarcity in islands and coastal areas of the Mediterranean (PRODIM) – Final Report to EC, 448p, CANaH Publication 6/08, Athens, pp 23–57
- Kogan FN (1995) Application of vegetation index and brightness temperature for drought detection. *Adv Space Res* 15:91–100
- Kogan FN (2001) Operational space technology for global vegetation assessment. *Bull Am Meteorol Soc* 82: 1949–1964
- Lanzl F, Richter R (1991) A fast atmospheric correction algorithm for small swath angle satellite sensors. ICO topical meeting on atmospheric, volume, and surface scattering and propagation, Florence, Italy
- Mulla DJ (2013) Twenty five years of remote sensing in precision agriculture: key advances and remaining knowledge gaps. *Biosyst Eng* 114(4):358–371
- Niemeyer S (2008) New drought indices, options Méditerranéennes. *Série A Séminaires Méditerranéens* 80:267–274
- Olesen JE, Bindi M (2002) Consequences of climate change for European agricultural productivity, land use and policy. *Eur J Agron* 16:239–262

- Psomiadis E, Dercas N, Dalezios NR, Spyropoulos NV (2016) The role of spatial and spectral resolution on the effectiveness of satellite-based vegetation indices. *Proc SPIE* 9998:99981L-1-13. <https://doi.org/10.1117/12.2241316>
- Psomiadis E, Dercas N, Dalezios RN, Spyropoulos N (2017) Evaluation and cross-comparison of vegetation indices for crop monitoring from Sentinel-2 and WorldView-2 images. *Proc SPIE* 10421:104211B. <https://doi.org/10.1117/12.2278217>
- Rafn EB, Contor B, Ames DP (2008) Evaluation of a method for estimating irrigated crop-evapotranspiration coefficients from remotely sensed data in Idaho. *J Irrig Drain Eng* 134:722–729
- Rouse JW, JrHaas RH, Deering DW, Schell JA, Harlan JC (1974) Monitoring the vernal advancement and retrogradation (green wave effect) of natural vegetation, greenbelt. MD NASA/GSFC Type III Final Report, pp 371
- Salehi B, Zhang Y, Zhong M (2012) The effect of four new multispectral bands of Worldview-2 on improving urban land cover classification. *ASPRS annual conference*, Sacramento, Ca, pp 7
- Sultan B, Gaetani M (2016) Agriculture in West Africa in the twenty-first century: climate change and impacts scenarios, and potential for adaptation. *Front Plant Sci* 7:1262. <https://doi.org/10.3389/fpls.2016.01262>
- Thenkabail PS, Gamage MSD, Smakhtin VU (2004) The use of remote sensing data for drought assessment and monitoring in Southwest Asia, research report. International Water Management Institute 85:1–25
- Tsakiris G, Vangelis H (2005) Establishing a drought index incorporating evapotranspiration. *European Water* 9-10:3–11
- Tsakiris G, Pangalou D, Vangeis H (2007) Regional drought assessment based on the reconnaissance drought index (RDI). *Water Resour Manag* 21(5):821–833
- Updike T, Comp C (2010) Radiometric use of WorldView-2 imagery. Technical Note, DigitalGlobe, 1601 Dry Creek Drwangle Suite 260 Longmont, Colorado, USA, 80503
- Varella CAA, Gleriani JM, dos Santos RM (2015) Chapter 9 – Precision agriculture and remote sensing. Sugarcane, pp 185–203. <https://doi.org/10.1016/B978-0-12-802239-9.00009-8>
- Calera A, Campos I, Osann A, D’Urso G, Menenti M (2017) Remote Sensing for Crop Water Management: From ET Modelling to Services for the End Users. *Sensors* 17(5):1104